

GT2011-45(' (

HEAT TRANSFER AND FRICTION FACTOR IN THE RIB ROUGHENED BLADE LEADING EDGE COOLING PASSAGE

Artem A. Khalatov

Institute for Engineering Thermophysics,
National Academy of Sciences of Ukraine
Kyiv City, Ukraine
E-mail: artem.khalatov@vortex.org.ua

Yuriy Y. Dashevskyy, Dmytro M. Pysmennyi

Gas Turbine Research & Production Complex
“Zorya”-“Mashproekt”
Mykolaiv City, Ukraine
E-mail: spe@mashproekt.nikolaev.ua

ABSTRACT

This paper presents the results of heat transfer and surface friction factor numerical simulation in the blade internal cooling passage with trip strip turbulators of different configurations and rib coverage. The passage cross section shape is the equilateral triangle with rounded apex simulating the leading edge area. The leading edge wedge angle is 30 degrees, inner radius to passage hydraulic diameter ratio is 0.30; channel hydraulic diameter is 10 mm. Such geometric parameters are typical to a leading edge cooling passage of an actual gas turbine blade or vane.

Totally six basic rib configurations have been studied including the continuous transverse ribbing (normal to bulk flow direction), V-shaped ribbing, inverted V-shaped ribbing, broken transverse ribbing, broken V-shaped ribbing, as well as helical ribbing (angled to the bulk flow direction). Three cases of the passage partial ribbing for the widely used transverse and V-shaped rib configurations have been also analyzed, and the smooth cooling passage of the same configuration and cross section have been studied for the reference comparison as well.

The ribs geometrical parameters for all configurations are the same: a square cross section, rib height to channel hydraulic diameter ratio (blockage ratio) is 0.10; rib pitch (rib-to-rib spacing) is 10, angle of attack for V-shaped, inverted V-shaped and helical ribs is 45°.

All calculations were carried out at the constant Reynolds number of 100 000 using commercial software package ANSYS CFX 11.0. The results presented in this paper include the heat transfer, surface friction, vortex structure analysis and thermal hydraulic performance evaluation.

INTRODUCTION

Development of convective cooling systems for advanced gas turbine blades and vanes is a very difficult engineering

problem. This is due to extremely high heat transfer from hot gas to the external turbine airfoil surface in the leading edge area, and a smaller heat transfer area of the cooling passage.

The trip strip technology is widely used for the internal blade cooling. The periodic ribbing destroys boundary layer and disturbs the near-wall flow area, thus increasing heat transfer. Over the last twenty years numerous studies on heat transfer and friction factor for rib-roughened channels were carried out [1-3]. Most of these studies were carried out for a square or rectangular cross section passage with two ribbed walls. However, such the configuration is typical for the central part of a blade cross section, therefore, the results obtained are not applicable for correct assessment of heat transfer in the leading edge area.

In [4, 5] heat transfer data were obtained in the passage of equilateral triangle cross-section with two ribbed walls and the analysis of the rib turbulator location effect on heat transfer was given. Results of these studies showed that rib inclination in the triangle and rectangular shape passage provided the heat transfer augmentation. The V-shaped rib configuration looks more preferable as providing greater heat transfer rate in the apex region, which simulates the blade leading edge.

Some investigations were aimed at studying of rotation effect on heat transfer in channels of different shape. The heat transfer data in the triangle passage at $X/D > 13$ from the inlet were presented in [6]. In [7, 8] heat transfer investigations were carried out in the same passage at $X/D < 7$. These studies revealed that rotation influenced significantly the heat transfer distribution in passage with transverse ribbing. For inclined ribs this effect is much lower. Numerical simulation of the rotation effect on heat transfer in the engine-similar two-pass internal cooling channel in the leading edge area was performed in [9]. The leading edge passage was of trapezoid cross section with V-

shaped ribs. According to these studies, the rotation influenced weakly the in-passage heat transfer.

Results obtained in the triangular shaped channel are different from those available in actual gas turbine blade with rounded leading edge. The cross section of the cooling passage investigated in [10], is closer to an actual leading edge shape; however only one rib configuration was investigated in this study.

The objective of the present study is the heat transfer investigation in the rounded leading edge area in the cooling passage with different rib turbulator configurations and with the cross section shape typical to a gas turbine airfoil. The effect of partial ribbing on heat transfer in the leading edge area and friction factor in the cooling passage was also investigated for most widely used rib configurations. Based on this data, the thermal hydraulic performance evaluation was performed.

NOMENCLATURE

- A – channel cross-section area;
- D – channel hydraulic diameter;
- e – rib height;
- f – friction factor;
- f_0 – friction factor found from the Blasius correlation;
- G – mass flow rate;
- k – air thermal conductivity;
- Nu – Nusselt number;
- Nu_0 – Nusselt number found from the Dittus-Boelter correlation;
- p – rib spacing;
- Pr – Prandtl number;
- q – specific heat flux;
- Re – Reynolds number;
- t_B – bulk flow temperature;
- t_w – wall temperature;
- X – distance from the passage inlet;
- x – cross section perimeter coordinate;
- α – rib angle of attack;
- ρ – air density;
- γ – leading edge wedge angle.

THP – thermal-hydraulic performance parameter.

Leading Edge Model

The basic passage geometry is shown in Fig. 1. The leading edge inner radius to passage hydraulic diameter ratio R/D is 0.3, leading edge wedge angle (γ) is 30° . Such geometrical parameters are representative to the cooling passage of actual gas turbine blade.

As found in previous investigations there are several rib parameters that influence greatly the heat transfer and surface friction, namely rib height to channel hydraulic diameter ratio (e/D), rib non-dimensional pitch in the flow direction (p/e), rib angle of attack (α). The previous studies have also shown that the best thermal-hydraulic performance parameter corresponds

to the following range of the non-dimensional parameters $0.06 < e/D < 0.10$ and $5 < p/e < 10$.

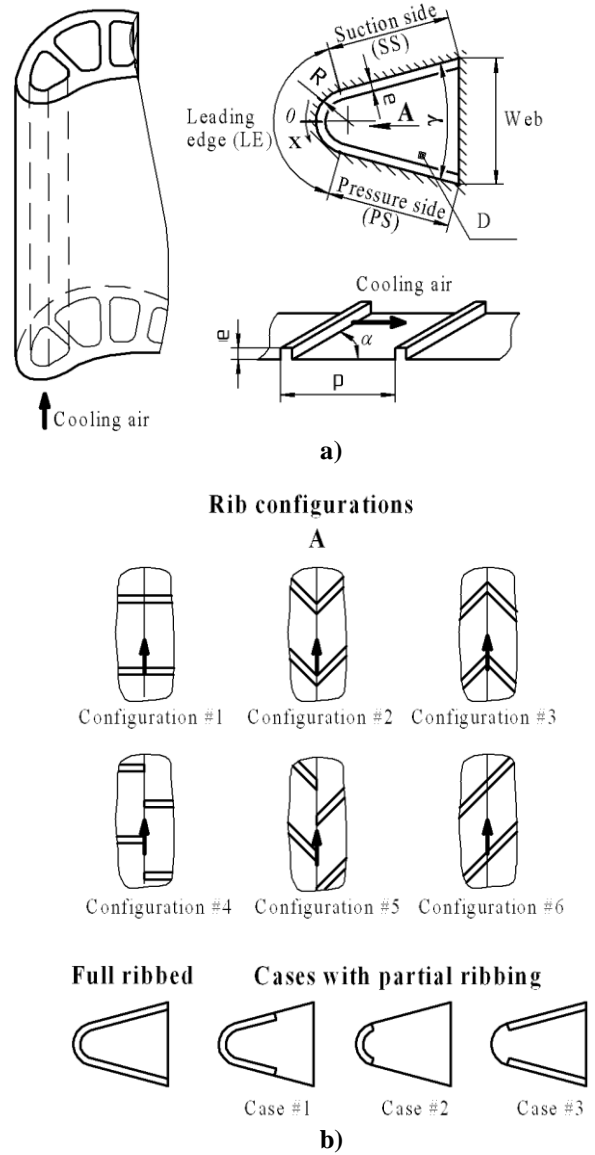


Figure 1. Passage and rib configurations
1– transverse ribbing, 2– V-shaped ribs, 3–inverted V-shaped ribs, 4– broken transverse ribs, 5–broken V-shaped ribs, 6–helical ribs. Partial ribbing: 1– ribbing over the leading edge and half-length side walls, 2– ribbing over the passage leading edge, 3– ribbing over the passage side walls.

All six ribbing configurations shown in Fig.1 were investigated in the present study. These configurations are of the identical rib geometry: square cross section, $e/D = 0.1$, $p/e = 10$, rib angle of attack for V-shaped, inverted V-shaped and helical rib $\alpha = 45^\circ$. The smooth passage of the same cross section was

also studied for comparisons as the reference passage configuration.

Three other ribbing configurations shown in Fig. 1.b were also studied to assess the effect of partial ribbing of the cross section. They include:

- case # 1: ribbing over the leading edge and over half-length side walls;
- case # 2: ribbing over the passage leading edge;
- case # 3: ribbing over the passage side walls.

All calculations were carried out at the constant Reynolds number Re of 100 000 which is typical to actual gas turbine blade operating conditions.

NUMERICAL PROCEDURE

Preliminary discussions

The Computational Fluid Dynamics (CFD) method was used to study heat transfer and friction factor in the periodically ribbed passage. The CFD-calculations were performed using commercial software package ANSYS CFX 11.0.

The passage cross-sectional area and flow parameters varied periodically in the streamwise direction, therefore the periodical approach was used for all calculations. This approach is typically employed for the flow numerical simulation in rib roughened cooling passages [10,11], so it can be used in the thermal stabilization area i.e. at the sufficient distance from the passage inlet. As found in [1], such the thermal stabilization appears at $X/D \geq 5$. Consequently, data obtained in the present study cannot be used for passage sections located at $X/D < 5$ from the inlet and in turn areas.

Prior to the basic research program to select the turbulence model the verification simulations were performed to assess heat transfer and surface friction in a smooth and rib roughened square and triangular cross section passages. The obtained results were compared with experimental data presented in [1, 6] and were discussed in details in [12].

The set of verification calculations was also performed in the periodical approach using the standard $k-\varepsilon$ turbulence model with scalable wall-function and low- Re SST turbulence model with automatic wall function. Both models use standard settings provided by ANSYS CFX and are widely used for the heat transfer calculations.

Comparisons of the verification and experimental data [1] for the smooth square passage and passages of the same cross section with transverse ribs and inclined ribs at the angle attack of 45° to the bulk flow direction led to the following conclusions:

- in case of smooth channel both turbulence models have demonstrated a good agreement with experimental data;
- for the transverse ribbing at $Re > 50\,000$ the SST turbulence model has underestimated heat transfer for the ribbed surfaces by 21% and for the friction factor in the passage by 40%; heat transfer simulations using $k-\varepsilon$ turbulence model

had spread with experimental data within 10%, while the friction factor data were in a good agreement with experiments;

– for the inclined ribs both turbulence models have demonstrated identical heat transfer difference from the experimental data of less than 10%; while the surface friction data obtained with SST turbulence model were in a good agreement with experimental data. The results obtained with $k-\varepsilon$ model have overestimated slightly the experimental data.

For both turbulence models at lower Reynolds numbers the difference between experimental data and computational results was more significant. The same results were obtained for the stationary triangle passage in [6]. Because of low Reynolds number ($Re=10\,000$) the difference between simulation and experimental data was greater.

In studies [11, 13] for transverse ribs the SST turbulence model was also used and the similar difference between experimental data and simulation results was obtained.

Taking into consideration this fact, $k-\varepsilon$ turbulence model was chosen for all simulations as it provided better agreement with experimental data for different rib configurations.

Domain

For each rib configuration the numerical domain of the same hydraulic diameter $D = 10$ mm was developed. The passage length was equal to two spacing between successive ribs.

Based on verification calculations, the standard $k-\varepsilon$ turbulence model with scalable wall-function was used for all calculations. In this model the values of turbulence kinetic energy (k) and turbulence eddy dissipation (ε) come directly from differential transport equations [14, 15]:

$$\frac{\partial(\rho k)}{\partial t} + \nabla(\rho U k) = \nabla \left[\left(\mu + \frac{\mu_t}{\sigma_k} \right) \nabla k \right] + P_k - \rho \varepsilon \quad (1)$$

$$\frac{\partial(\rho \varepsilon)}{\partial t} + \nabla(\rho U \varepsilon) = \nabla \left[\left(\mu + \frac{\mu_t}{\sigma_\varepsilon} \right) \nabla \varepsilon \right] + \frac{\varepsilon}{k} (C_{\varepsilon 1} P_k - C_{\varepsilon 2} \rho \varepsilon) \quad (2)$$

Here μ_t is the turbulence viscosity. $C_{\varepsilon 1}$, $C_{\varepsilon 2}$, σ_k and σ_ε are model constants. P_k is the turbulence production due to viscous and buoyancy forces. The scalable wall-function within ANSYS CFX approach is introduced to improve robustness and accuracy when the near-wall mesh is very fine.

The following boundary conditions were used for calculations: the constant wall temperature $t_w = 800$ °C was imposed to all surfaces; to provide the periodicity, the translational-periodic boundary conditions including pressure change target at the inlet and outlet were used; the volumetric heat sink Q , providing the periodicity of temperature field and calculated as the total heat flux from the channel wall, related to the numerical domain volume, was used for the whole domain.

The average static pressure in the domain was about 1 MPa, the in-passage pressure drop was variable to provide the air mass flow rate corresponding to the Reynolds number of 100 000, while the inlet bulk flow temperature was 500 °C for all calculations.

The hexahedral structured grids were generated by the commercial software package ANSYS ICEM CFD 11.0. For each domain two grids were generated. Coarse grid included from 100 000 to 200 000 cells, the fine grids included from 500 000 to 700 000 cells. For all cases studied the value of dimensionless distance between the wall and the first grid node (y^+) varied from 5 to 10 to satisfy the $k-\varepsilon$ model with scalable wall-function requirements. As an example, the numerical domain and element of grid for the rib configuration # 2 are shown in Fig. 2.

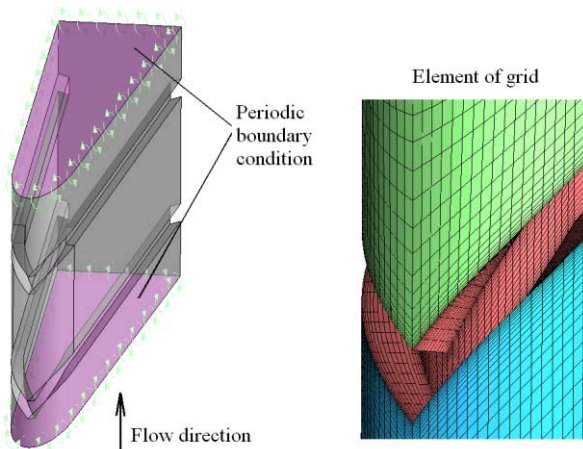


Figure 2. Numerical domain and grid element

For all variants, calculations were performed with the use of coarse and fine grids for grid independence control. All computations were carried out for steady state conditions and considered converged when the root mean square residual for the energy equation had decreased by 10^{-6} , and by 10^{-5} for other equations. Furthermore, integrated quantities, e.g. mass flow rate and area-averaged heat transfer coefficients were monitored and used as more strict convergence criteria.

Data processing

The heat transfer rate through the channel walls was determined using the Nusselt number Nu . The values of Nu number were obtained as a result of flow simulations, according to the specific heat fluxes (q) distribution:

$$Nu = \frac{D}{k} \frac{q}{t_w - t_B} \quad (3)$$

Here k is the air thermal conductivity; D is the passage hydraulic diameter; t_w is the wall temperature; t_B is the bulk flow temperature.

To assess the heat transfer augmentation rate all Nusselt numbers were normalized using the Nu_0 reference number obtained from the Dittus-Boelter correlation for the fully developed turbulent flow in a smooth round tube:

$$Nu_0 = 0.023 \cdot Re^{0.8} \cdot Pr^{0.4} \quad (4)$$

The in-passage pressure drop was calculated according to the correlation:

$$f = \frac{\Delta P^* \rho D A^2}{2 p G^2} \quad (5)$$

where ΔP^* is the total pressure drop at ribs spacing; ρ is the air density; A is the channel cross section area; G is the air mass flow rate; p is the axial pitch (Fig. 1).

For further comparisons the friction factor was normalized using the Blasius reference correlation for the fully developed turbulent flow in a smooth circular tube:

$$f_0 = 0.079 \cdot Re^{-0.25} \quad (6)$$

In correlations (3), (4), (6) Reynolds number is based on the channel hydraulic diameter and channel average axial flow velocity.

The thermal-hydraulic performance (THP) was evaluated as $(Nu/Nu_0)/(f/f_0)^{1/3}$. This non-dimensional parameter is the ratio of heat transfer augmentation rate in the ribbed channel to the associated increase of the friction loss at the identical pumping power.

DATA ANALYSIS: FULLY RIBBED CHANNEL

Heat transfer

The heat transfer analysis was performed for four typical passage areas, presented in Fig. 1. For each of them the axially averaged and perimeter averaged Nusselt numbers were used. The Nusselt numbers were normalized using the smooth channel data (Nu_0) calculated from the correlation (4). The additional heat transfer surface due to ribbing was taken into consideration for all Nu number calculations.

The normalized Nu/Nu_0 ratios for the smooth and ribbed passages are presented in Table 1. In the smooth passage the perimeter averaged Nusselt number is 9% lower than that calculated from the correlation (4). This result represents the passage shape effect and is in a good agreement with experimental data obtained in the similar passage [10]. Actually the same results were obtained in the rectangular passage [16].

Figure 3 presents the axially averaged Nu/Nu_0 ratios versus the perimeter coordinate x (Fig. 1), normalized to the leading edge inner radius R . Figure 4 presents the local Nu/Nu_0 ratios for the smooth surface between sequential ribs.

As seen, at the identical e/D and p/e values the rib configuration influences greatly the local and average heat

transfer distribution. Even in the smooth passage, because of the non-circular cross section, significant heat transfer non-uniformity occurs in the angular direction: in particular, in the leading edge area of the smooth passage the average Nusselt number is 15% lower than that, calculated from the correlation (4).

Table 1. Fully ribbed passage: Nu/Nu_0 ratio and THP parameter

	Nu/Nu_0				f/f_0	$\frac{Nu/Nu_0}{(f/f_0)^{0.33}}$	
	Region			Perimeter averaged		LE	Perimeter averaged
	LE	SS & PS	Web				
<i>Smooth channel</i>	0.84	0.95	0.86	0.91	0.97	0.85	0.91
Config. 1	2.21	2.76	2.03	2.46	19.11	0.83	0.92
Config. 2	3.70	3.17	1.98	2.94	18.72	1.39	1.11
Config. 3	1.96	3.40	2.28	2.83	18.61	0.74	1.07
Config. 4	2.80	2.70	1.99	2.53	19.21	1.05	0.94
Config. 5	4.02	3.02	1.95	2.92	17.11	1.56	1.13
Config. 6	1.78	2.26	1.59	1.99	6.92	0.93	1.04

In the leading edge area the greatest heat transfer augmentation rate for the V-shaped ribs (configurations # 2 and # 5) is in a good agreement with results obtained in [4 - 6]. In these configurations the average normalized Nusselt number in the leading edge area is 3.70 and is 4.02, correspondingly. Most low Nu/Nu_0 ratios in the leading edge area were registered for the inverted V-shaped ribs (configuration # 3) and for the helical ribs (configuration # 6). The lowest perimeter averaged heat transfer augmentation rate was obtained for the configuration # 6, while the greatest heat transfer augmentation rate over the smooth web (partition wall) was registered for configuration # 3.

The flow disturbance caused by “rib breaking” provides heat transfer growth in the leading edge by 26% for the transverse ribbing and by 9% for the V-shaped ribbing. As seen from Fig. 4, for the broken V-shaped ribbing the local maximum of Nu/Nu_0 ratio is slightly lower than that obtained for the continuous V-shaped ribs in the rib apex downstream zones. For the broken transverse ribbing the maximum values of the Nu/Nu_0 ratio occurred in the leading edge area increase, as well.

The “step-like” drop in the normalized Nusselt numbers occurred at the border between ribbed pressure side and suction side and cylindrical ribbed portion of the leading edge (Fig. 3) can be explained by decrease in the ribbing factor from 1.2 to 1.13 for the transverse ribs and from 1.28 to 1.21 for the V-shaped ribs.

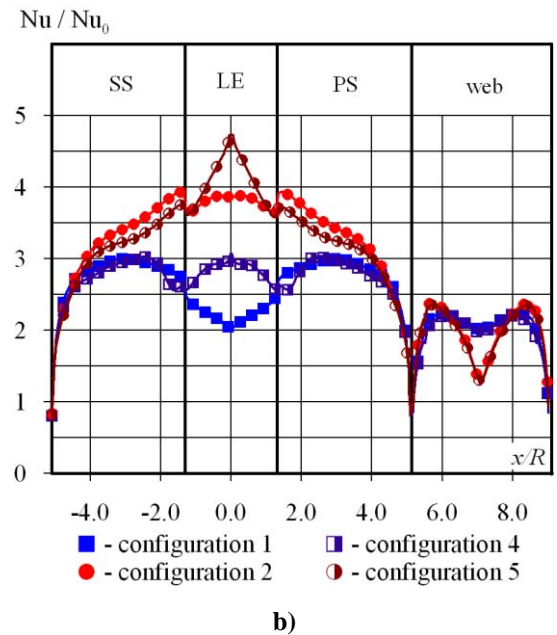
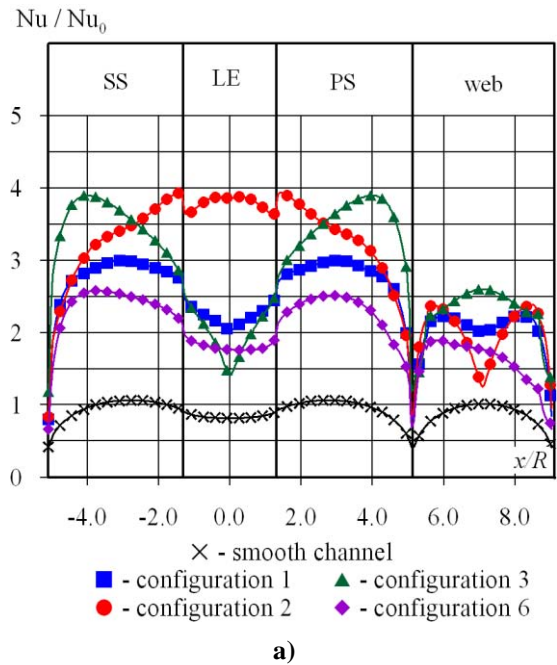


Figure 3. Axially averaged Nu/Nu_0 ratio vs. the perimeter coordinate x

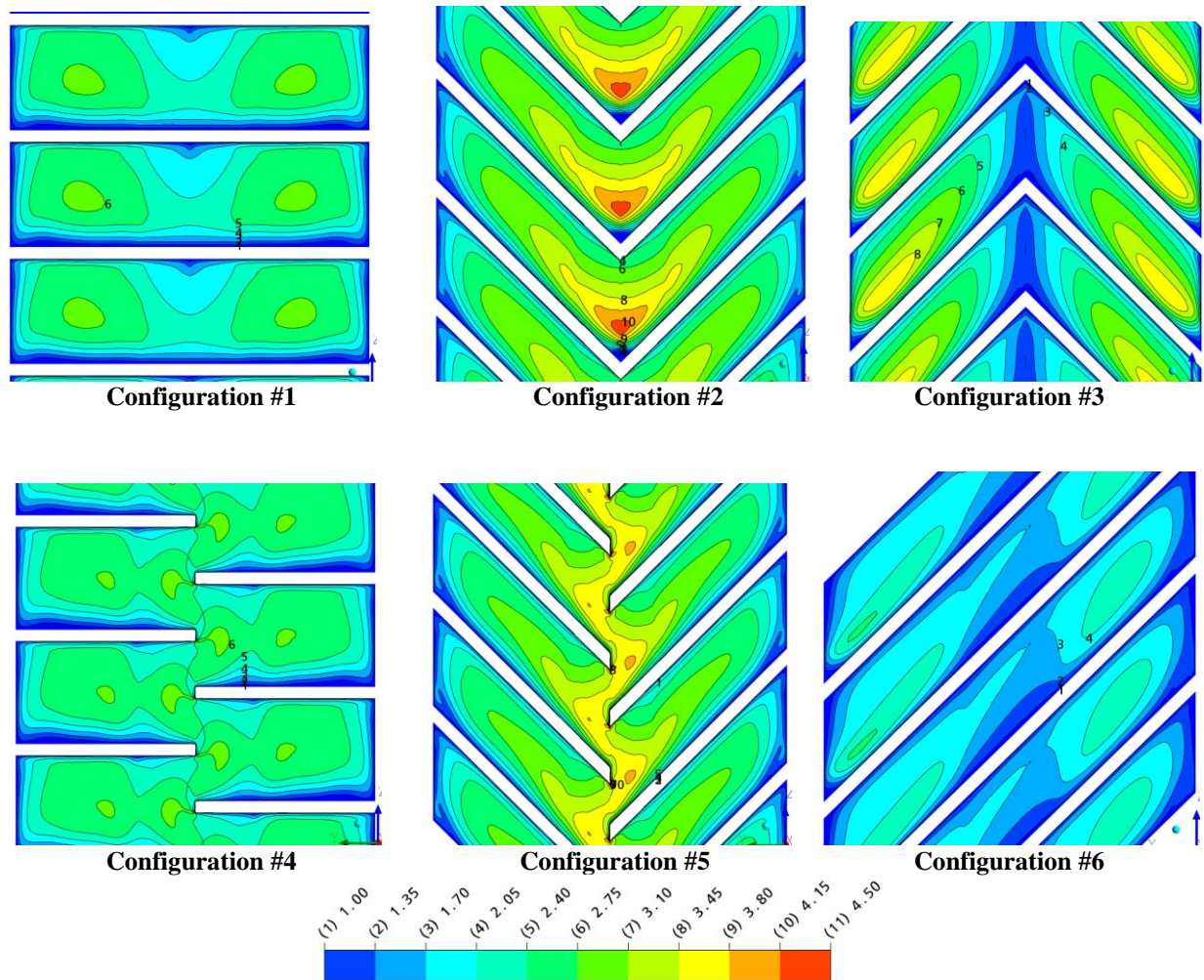


Figure 4. Fully ribbed passage: Nu/Nu_0 isolines for various configurations

When analyzing the flow structure in ribbed passage, the heat transfer distribution over channel cross section is primarily characterized by secondary flows, caused by the ribs. These secondary flows for the V-shaped and inverted V-shaped rib configurations have the form of the twin-vortex structures. Distribution of velocity vectors in the channel cross section for V-shaped and inverted V-shaped ribs and twin vortex structure are shown in Fig. 5. In the first case the formed vortices transfer more cold flow from the core towards the leading edge area. In the second case this flow moves towards the un-ribbed web, but the heated flow moves from the channel side walls to the leading edge area. The helical ribbing (configuration # 6) induces single vortex in the passage cross section swirled to the rib direction. In case of transverse ribbing (configuration # 1) there are no secondary flows, affecting the heat transfer.

Taking into consideration the vortex flow structure, the distribution of axially averaged Nusselt number ratios (Nu/Nu_s), rated to the smooth passage of the same cross section shown in Fig. 6 is of specific interest. For the transverse ribbing (# 1) and helical ribbing (# 6) the Nu/Nu_s ratio changes slightly with some decrease near the leading edge area due to reduction in the ribbing factor. Rather sharp Nu/Nu_s growth in the leading edge area for the V-shaped ribs is explained by the twin vortex presence. For the inverted V-shaped ribs the twin vortex causes more significant Nu/Nu_s ratio drop down in this area.

Figure 7 presents the non-dimensional (normalized) axial flow velocities averaged in axial direction. The cross section averaged axial velocity speed was taken as the reference parameter. As seen from this figure, the transverse ribs (# 1) transfer the flow core towards un-ribbed web (partition wall), thus providing minimal flow speed in the leading edge area.

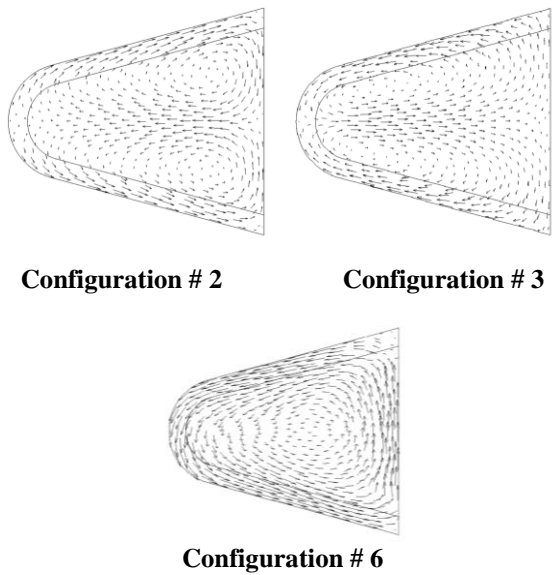


Figure 5. Secondary flow pattern in the passage cross section

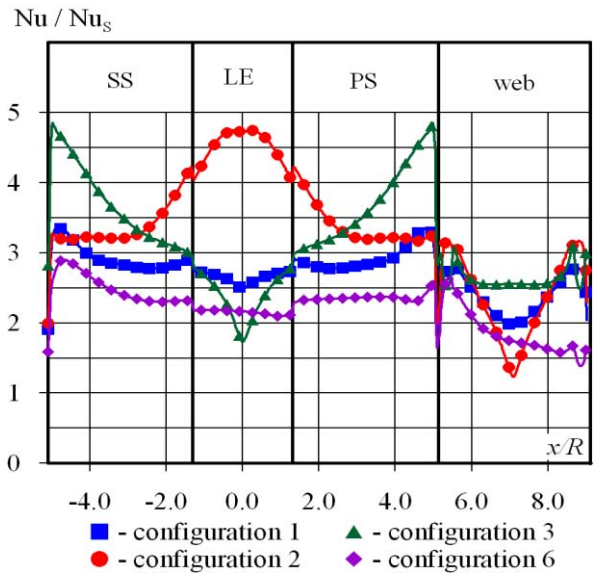


Figure 6. Axially averaged Nu/Nu_0 ratio over the passage perimeter coordinate x

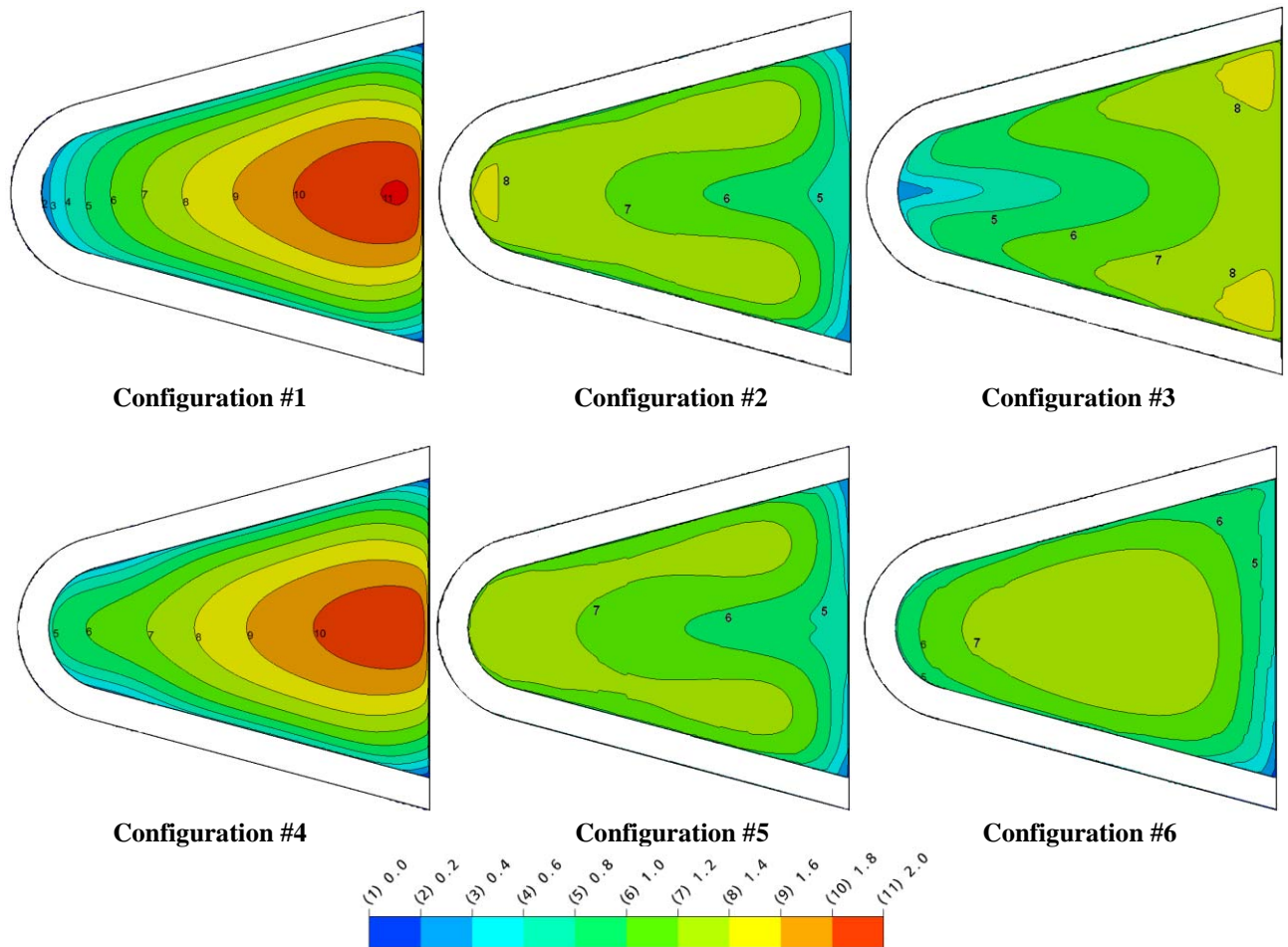


Figure 7. Fully ribbed passage: normalized axially averaged axial velocity field for different configurations

Friction factor

The normalized friction factors (f/f_0) for all investigated configurations are presented in Table 1. As seen, configurations # 1-5 are of approximately identical f/f_0 values ranging from 17.11 to 19.21. For the configuration # 6 with helical ribbing, which does not generate twin vortex structure, it is significantly lower ($f/f_0=6.92$). It means that at the identical air mass flow rate the inclined rib configurations provide much lower pressure drop than transverse, V-shaped and inverted V-shaped ribs. The Nu/Nu_0 ratio for configuration # 6 is also lower than that for configurations # 1-5 both in the leading edge area and in the whole passage.

In the smooth channel $f/f_0=0.97$ i.e. by 3% lower than that calculated from equation (6). This result also represents the passage shape effect and is in a good agreement with experimental data obtained in the passage of similar cross section [10].

Thermal-hydraulic performance

The THP parameter $(Nu/Nu_0)/(f/f_0)^{0.33}$ data both in the leading edge area and the whole passage are also given in Table 1. As seen, for all rib configurations studied the perimeter averaged THP parameter is greater than that obtained in the smooth passage.

As for the leading edge area, the THP parameter for the configurations # 1 and # 3 is slightly lower than that for the smooth passage. The maximum values of the THP parameter both for the leading edge area and the whole passage demonstrates the configuration # 5, while the configuration # 2 provides the lowest magnitude of THP parameter.

PARTIALLY RIBBED PASSAGE

For the widely used transverse (configuration #1) and V-shaped rib configurations (configuration #2), three different cases (Fig. 1) of the passage cross section partial ribbing were studied.

Distribution of axially averaged normalized Nusselt number over the channel cross section is presented in Fig. 8. The Nu/Nu_0 ratios for four specific areas and the whole channel cross section are presented in Table 2. Normalized local Nusselt number distribution over the smooth surface for three cases is presented in Fig. 9. Fig. 10 presents the non-dimensional axially averaged normalized axial velocity fields. The cross section averaged axial flow velocity is used as the reference parameter.

Case # 1. For the transverse ribs the partial ribbing, in comparison to the full ribbing, leads to reduction by 31% in the heat transfer rate in the leading edge area. For the V-shaped rib configuration, the heat transfer decrease over the leading edge is about 8%. As seen from Fig. 8, decrease in the heat transfer over the ribbed portion of side walls is insignificant, but average heat transfer values for side walls are significantly lower (Table 1).

Table 2. Partially ribbed passage: Nu/Nu_0 ratio and THP parameter

	Nu/Nu ₀				f/f ₀	Nu/Nu ₀ (f/f ₀) ^{0.33}	
	Regions			Perimeter averaged		LE	Perimeter averaged
	LE	SS & PS	Web				
Fully ribbed channel							
Config. 1	2.21	2.76	2.03	2.46	19.11	0.83	0.92
Config. 2	3.70	3.17	1.98	2.94	18.72	1.39	1.11
Case # 1							
Config. 1	1.52	1.84	1.36	1.65	5.88	0.84	0.91
Config. 2	3.41	2.49	1.33	2.34	11.68	1.51	1.03
Case # 2							
Config. 1	1.40	1.23	1.03	1.20	2.12	1.09	0.94
Config. 2	2.17	1.15	0.96	1.29	2.62	1.58	0.93
Case # 3							
Config. 1	1.63	2.49	1.75	2.13	12.79	0.70	0.91
Config. 2	2.22	3.16	1.86	2.62	13.77	0.93	1.10

The reduction of the ribbed portion decreases the surface friction, especially for the transverse rib configuration. In this case the normalized friction factor f/f_0 is 5.88 for transverse ribbing and 11.68 for the V-shaped ribbing. For the full ribbing case these values are 19.11 and 18.72 correspondingly.

The V-shaped rib configuration also demonstrates better THP parameter than transverse ribbing both in the leading edge area and the whole channel (perimeter averaged). In the leading edge area for the V-shaped ribs THP parameter is 1.51, while for the transverse ribs THP is 0.84.

Case # 2. In this case, heat transfer in the leading edge area decreases significantly for both configurations. The V-shaped ribs demonstrate an advantage in terms of the heat transfer rate ($Nu/Nu_0 = 2.17$) in comparison to transverse ribs ($Nu/Nu_0 = 1.40$). For the full ribbing case these values are 2.21 and 3.70 correspondingly. As seen from Fig. 10, the transverse ribs displace the air flow from the leading edge towards the web more remarkably than the V-shaped ribs. Due to this reason, the Nusselt numbers for the transverse ribs over the leading edge area are close to those for the smooth side surfaces, despite the increase in the heat transfer surface.

The normalized friction factor f/f_0 for the transverse and V-shaped ribbing is 2.12 and 2.62, correspondingly.

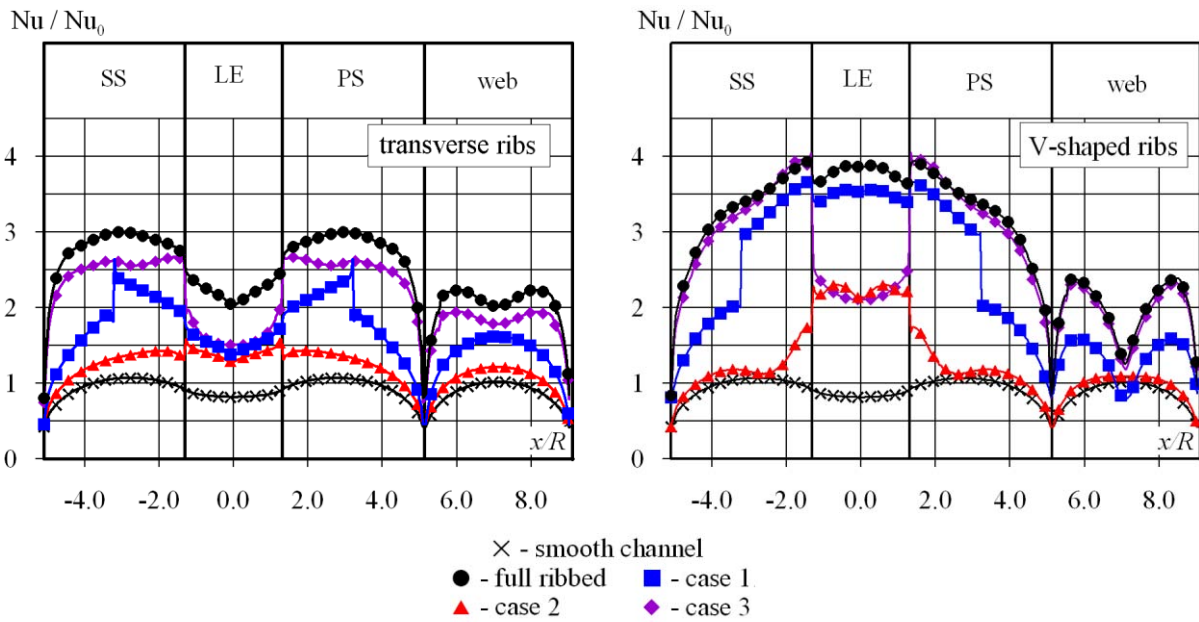


Figure 8. Partially ribbed passage: axially averaged Nu/Nu_0 ratio over the passage perimeter coordinate x

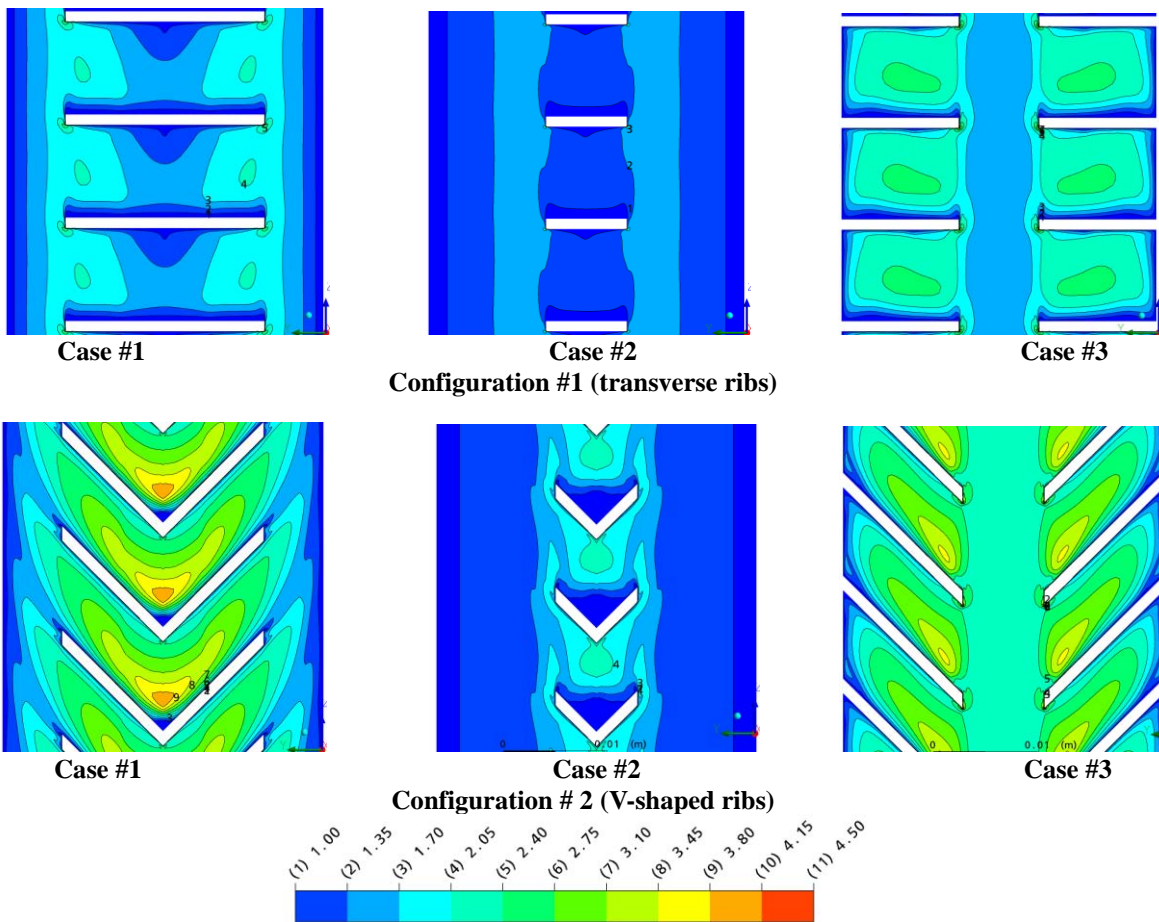


Figure 9. Partially ribbed passage: Nu/Nu_0 isolines for different cases

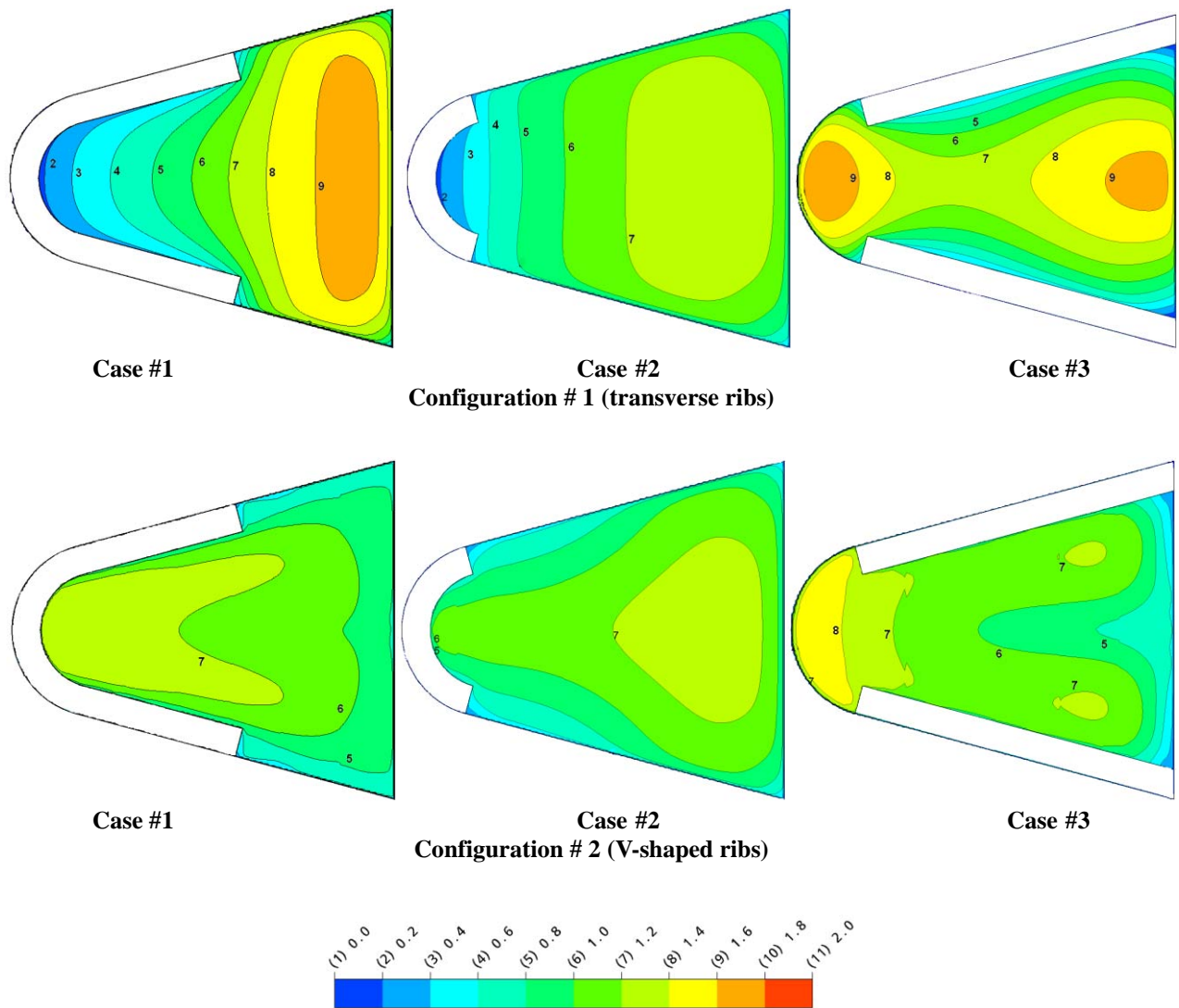


Figure 10. Partially ribbed passage: normalized axially averaged axial velocity field for different cases

In the leading edge area for the V-shaped ribs THP parameter is 1.58 which is significantly greater than that for the transverse ribbing where THP is 1.09.

Case #3. For the transverse rib configuration, compared to full ribbed passage, the Nu/Nu_0 ratio is by 10% lower on the ribbed walls and by 26% lower in the leading edge area. This is due to reduction in the heat transfer area (no ribs). As seen from Fig. 10, two zones of higher flow velocity exist near the leading edge and close to the un-ribbed web center.

For the V-shaped ribbing the Nu/Nu_0 ratio on the ribbed side walls is equal to the full ribbing case. However, the Nu/Nu_0 ratio at the leading edge reduces from 3.70 to 2.22, i.e. by 40% in comparison to the full ribbing case.

In this case, the normalized friction factor f/f_0 is 12.79 for the transverse ribbing and is 13.77 for the V-shaped ribs. These values are much greater than that available for the case #1 and case #2.

For the transverse ribs in the leading edge area THP parameter is 0.70 which is the lowest one in comparison to all other cases. For the V-shaped ribs the THP parameter in the leading edge area is greater (THP = 0.93). However, it is much lower than the data obtained in case # 1 (1.51) and case # 2 (1.58). The perimeter averaged THP is 1.10 and is greater than that one for the case # 1 (1.03) and case # 2 (0.93).

CONCLUSIONS

Numerical simulations were performed to study heat transfer and surface friction in the triangular shape cooling passage with rounded apex and trip strip turbulators of various configurations and rib coverage. For all investigated variants, THP parameters were also evaluated. The following basic conclusions can be drawn from this study results.

1. In the full ribbing case the greatest heat transfer rate and best THP factor demonstrate the V-shaped and broken V-shaped ribbing both in the leading edge area and whole channel cross section (perimeter averaged). Compared with continuous ribbing the broken ribs provide further heat transfer enhancement in the leading edge area, while the perimeter averaged heat transfer is actually the same for broken and continuous ribs. Helical ribbing demonstrates the lowest heat transfer in the leading edge area.

2. The heat transfer distribution along the perimeter depends greatly on the twin vortex structures existing in the passage, especially for the V-shaped and inverted V-shaped rib configurations.

3. Reduction of the side wall ribbing length (case # 1 and # 2) decreases heat transfer in all passage areas in comparison to the full ribbing case (mostly for the transverse ribbing).

For the case of no ribbing in the leading edge area (#3), the V-shaped and transverse ribbing demonstrate greater heat transfer than in case of the leading edge ribbing (#2).

For all cases of the partial ribbing the V-shaped ribbing in the leading edge area provides significantly greater heat transfer rate than the transverse ribbing

ACKNOWLEDGMENTS

The authors gratefully acknowledge Mr. O. Nikolashchenko, Ms. V. Levert and Mrs. S. Tsvihun for their support in this paper preparation.

REFERENCES

[1] Han J.C., Park J.S., Lei C.K. "Heat transfer enhancement in channels with turbulence promoters", ASME J. Engine gas turbines Power, 1985, Vol. 107, pp. 629–635.

[2] Lau S.C., Kukreja R.T., McMillin R.D. "Effect of V-shaped rib arrays on turbulent heat transfer and friction of fully developed flow in a square channel" Journal Heat Mass Transfer, 1991. Vol. 34, No. 7, pp. 1605–1616.

[3] Taslim M.E., Li T., Kercher D.M., "Experimental heat transfer and friction in channels roughened with angled, V-shaped and discrete ribs on two opposite walls", 1994, ASME Paper 94-GT-163.

[4] Metzger, D. E., Vedula, R., and Breen, D. D., "The effect of rib angle and length on convection heat transfer in rib-roughened triangular ducts", 1987. Proc. ASME-JSME Thermal Engineering Joint Conference, Vol. 3, pp. 327–333.

[5] Metzger, D. E., and Vedula, R., "Heat transfer in triangular channels with angled roughness rib on two walls", 1987. Experimental Heat Transfer, Vol. 1, pp. 31–44.

[6] Lee D.H., Rhee D.H., Cho H.H. "Heat transfer measurements in a rotating equilateral triangular channel with various rib arrangements", 2006. ASME Paper GT2006-90973.

[7] Liu Y-H., Huh M., Rhee D-H., Han J-C., Moon H-K. "Heat transfer in leading edge, triangular shaped cooling channels with angled ribs under high rotation numbers", 2008. . ASME Paper GT2008-50344.

[8] Liu Y-H., Han J-C., Huh M., Moon H-K. "High rotation number effect on heat transfer in a triangular channel with 45°, inverted 45°, and 90° ribs", 2009. ASME Paper GT2009-59216.

[9] Schuler M., Dreher H.-M., Neumann S.O., Weigand B, Elfert M. "Numerical predictions of the effect rotation on fluid flow and heat transfer in an engine-similar two-pass internal cooling channel with smooth and ribbed walls", 2010, ASME Paper GT2010-22870.

[10] Domaschke N., Wolfersdorf J., Semmler K. "Heat transfer and pressure drop measurements in a rib roughened leading edge cooling channel", 2009. ASME Paper GT2009-59399.

[11] Walker D., Zausner J. "RANS evaluations of internal cooling passage geometries: ribbed passages and a 180 degree bend", 2007, ASME Paper GT2007-27830.

[12] Pysmennyi D. "CFD simulation of heat transfer and pressure drop in a rib-roughened channel". Herald of aeroenginebuilding. – 2009. – №3 (22).– pp. 82–87.

[13] Chen W., Ren J., Jiang H. "Verification of RANS for analyzing convective cooling system with and without ribs", 2009. ASME Paper GT2009-59427.

[14] Turbulence and Near-Wall Modeling / ANSYS CFX-Solver Modeling Guide /ANSYS CFX Release 11.0, ANSYS Europe Ltd. 2006. P. 97-132

[15] Turbulence and Wall Function Theory /ANSYS CFX-Solver Theory Guide / ANSYS CFX Release 11.0, ANSYS Europe Ltd. 2006. P. 69-118.

[16] Maurer M., Wolfersdorf J., Gritsch M. "An experimental and numerical study of heat transfer and pressure losses of V- and W-shaped ribs at high Reynolds numbers", 2007. ASME Paper GT2007-27167.